J Mater Sci (2011) 46:3084–3093
DOI 10.1007/s10853-010-5187-8

Investigation of surface properties of plasma-modified polyamide 6 and polyamide 6/layered silicate nanocomposites

Qi Zhou · Kean Wang · Leslie S. Loo

Received: 12 October 2010 / Accepted: 10 December 2010 / Published online: 23 December 2010

Abstract Polyamide 6 and polyamide 6/layered silicate nanocomposites were treated by oxygen plasma and the resulting surfaces were characterized by X-ray photoelectron spectroscopy (XPS) and Fourier transform infrared-attenuated total reflection (FTIR-ATR). The surface properties were also analyzed by water contact angle measurements and Taber abrasion test. It is found that plasma treatment had different effects on the surfaces of the homopolymer and the polymer nanocomposites. Furthermore, both plasma duration and nanoclay content affect the contact angle and degree of abrasion resistance. In pure polyamide 6, plasma treatment caused the surface to be highly hydrophilic due to the formation of cyclic *cis*-amide species. Polymer nanocomposites treated with plasma also became more hydrophilic due to oxidation and enrichment of clay at the surface. The abrasion resistance of pure polyamide 6 was increased after exposure to plasma. This is attributed to cross-linking of polymer chains when exposed to plasma. For the polymer nanocomposites, an improvement in abrasion resistance was obtained in samples with low clay content when exposed to plasma for a short time. This is also due to cross-linking as well as the higher abrasion resistance of clay. However, longer exposure to plasma resulted in poorer abrasion resistance due to self-aggregation of clay particles which can be easily removed from the surface. A model was proposed to explain the effect of oxygen plasma on polymer nanocomposite surface.

Q. Zhou · K. Wang · L. S. Loo (✉)
School of Chemical and Biomedical Engineering, Nanyang Technological University, Singapore 637459, Singapore
e-mail: SSLoo@ntu.edu.sg

Introduction

Polymer-layered silicate nanocomposites (PLSNs) have attracted a great deal of attention in both academia and industry since the Toyota research group first successfully synthesized polyamide 6/montmorillonite (MMT) nanocomposites [1]. Much research work have since been devoted to synthesizing or preparing hybrids based on other polymers or nanofillers [2]. In many cases, the PLSNs demonstrated enhanced mechanical, thermal, electrical, and barrier properties as compared to the homopolymers and micro-composites [3, 4].

Though a great deal of effort has focused on the bulk properties of PLSNs, their surface properties (e.g., abrasion resistance, hydrophilicity, etc.) have received less attention [4]. The addition of a second inorganic phase into homopolymers offers new possibilities, not only in enhancing the bulk properties of the resulting nanocomposite, but also in customizing suitable surface properties for different applications.

Polyamide 6 is an important engineering plastic used widely in applications such as bearings and gears where high abrasion resistance is critical. In the early 1990s, the Toyota research group successfully synthesized polyamide 6/montmorillonite nanocomposites with excellent tensile, thermal, and barrier properties [5]. However, polyamide 6/MMT nanocomposites were found to have poor abrasion performance. Srinath and Gnanamoorthy showed that melt intercalated polyamide 6 nanocomposites exhibited lower abrasion resistance compared to the homopolymer [6, 7]. In a further study, our group was able to investigate the micro-mechanics of the abrasion process in polymer nanocomposites using Fourier transform infrared (FTIR) and X-ray photoelectron spectroscopy (XPS) techniques [8].

Plasma treatment of surfaces is a well-developed technique to produce controlled surface modification of polymers [9]. A plasma is a cluster of particles containing equal numbers of positive ions and electrons, free radicals, and natural species created by exciting a gas in an electromagnetic or electrical field [10]. The presence of these species induces the formation of free radicals in the polymeric chains and hence serves to activate the polymeric surface [11]. The gas composition and plasma conditions will determine the type of reactions occurring on the polymer surface, e.g., etching, activation, functionalization, chain scission, or cross-linking [12]. Such plasma treatment of polymeric materials can lead to enhanced properties such as adhesion, durability, wettability, biocompatibility, and friction resistance [12, 13]. In contrast to polymers and other organics, inorganic materials such as nanoclay are much more stable when exposed to oxygen plasma [14].

There are only a handful of reports on the surface modification of PLSNs by plasma. Fong et al. [15] exposed both polyamide 6/MMT and epoxy/MMT nanocomposite surface to oxygen plasma. As a result, a passivated inorganic surface region was formed at the polymer nanocomposite surface due to the preferential removal of organics. The authors concluded that this inorganic layer retarded penetration of the plasma and prevented further polymer degradation. Wu et al. [16, 17] have used a mixture of oxygen (O_2) and nitrogen (N_2) plasmas to modify the surface of polyethersulfone/layered silicate nanocomposites and cyclic olefine copolymer/layered silicate nanocomposites. They found no difference in the surface roughness and barrier properties of both the homopolymers and the nanocomposites after plasma modification.

To the authors' knowledge, the abrasion resistance of PLSNs treated with plasma has not been investigated previously. In this work, pure polyamide 6 and its nanocomposites have been modified by oxygen plasma. The surface chemical structure changes were investigated by XPS and FTIR spectroscopy. The properties of the surfaces were then discussed in light of the surface structure.

Experimental

Materials

Polyamide 6 (PA) films and polyamide 6/montmorillonite nanocomposite films containing 2, 4, 6, and 8 wt% nanoclay (designated as PC2, PC4, PC6, and PC8, respectively) were purchased from Nanocor Corporation and used as received. The nanocomposites were made by in situ polymerization of polyamide 6 with 12-aminododecanoic acid-modified montmorillonite and then melt extruded. The thickness of the films ranged from 0.06 to 0.08 mm.

Surface treatment by O_2 plasma

O_2 plasma treatment was carried out in a March PX-500 lead frame plasma cleaning system operating at a radio frequency of 13.56 MHz. The glow discharge was produced using a plasma power of 400 W and O_2 flow rate of 150 sccm (standard cubic centimeters per minute). Plasma duration times were set at 15, 30, 45, and 60 min, respectively. After the plasma treatment, the samples were stored under ambient conditions (i.e., at a temperature of 23 °C and relative humidity of 65%).

X-ray photoelectron spectroscopy

X-ray photoelectron spectroscopy measurements were made using a Kratos Ultra XPS system equipped with an Al $K\alpha_{1,2}$ X-ray source ($h\nu = 1486.6$ eV). The pressure in the analysis chamber was maintained at or below 3.0×10^{-9} Torr during the measurements. The spectra were obtained at a photoelectron take-off angle of 90° measured with respect to the plane of the sample surface. Peak fitting was performed using a Shirley baseline. The areas of the XPS peaks were divided by the instrument relative sensitivity factor to account for the different photoionization cross-sections.

Infrared spectroscopy

Fourier transfer infrared-attenuated total reflection measurements were performed on a Nicolet Nexus 5700 spectrometer using the Smart Orbit ATR accessory. The beam splitter was KBr and the detector was a liquid nitrogen-cooled MCT detector. 64 scans were collected for each spectrum at a resolution of 2 cm^{-1}. ATR correction was applied to each spectrum.

Abrasion test

Abrasion tests were performed on a Taber model 5135 Abraser under atmospheric conditions. The loading was set at 1000 g and two CS-17 Calibrase abrasion wheels were used to effect the abrasion. 1000 cycles were performed on each sample. The weight loss during this process was taken as the measure of abrasion resistance. Three samples were tested for each material, and the results were then averaged.

Contact angle measurement

Water contact angles were measured by the sessile drop method on an FTA200 Dynamic Contact Angle Analyzer. A drop of ultrapure water was deposited on the sample surface, and the contact angle was determined by the equipment software. At least three measurements per

sample were taken. Ultrapure water (8.02 MΩ cm) was obtained from Millipore Milli-Q system.

Results and discussion

Plasma-treated polyamide 6

Changes in the surface chemistry of the samples were analyzed using XPS and ATR measurements. Table 1 shows the XPS atomic concentration analysis results of untreated and plasma-treated PA films. It is observed that after plasma treatment, the relative atomic concentration of oxygen increases about twofold, while the concentrations of carbon and nitrogen atoms decrease. Furthermore, the atomic composition does not vary significantly with increasing plasma duration, indicating that the surface composition has reached steady state after 15 min of plasma treatment.

Further analysis was performed on the chemical components of C 1s. Figure 1 shows the XPS C 1s spectra of pure polyamide 6 before and after plasma treatment. The C 1s spectrum of untreated PA in Fig. 1a has been fitted with four peaks [18]. The C–C peak (C1) is attributed to the carbon atoms of methylene groups in the main chain and its binding energy is calibrated to 284.6 eV. The *C*–C=O peak (C2) at 285.2 eV represents the carbon atom bonded to the carbonyl carbon of the amide group. The C–N/C–O peak (C3) at 286 eV is generally attributed either to the carbon atom bonded to the amide nitrogen or to the carbon atom bonded to alcohol or ether groups formed due to oxidization reactions. The N–C = O peak (C4) at 287.7 eV is assigned to the carbonyl carbon of the amide group.

Figure 1b shows a representative XPS C 1s spectrum of polyamide 6 after 60 min of O_2 plasma treatment. All the plasma-treated PAs have qualitatively similar C 1s spectra regardless of the plasma duration. It was found that a total of five peaks were necessary to fit the spectra of plasma-treated PA. Four of these peaks are similar to those of the untreated PA. The additional new peak (C5) is located at

Table 1 XPS atomic concentration analysis of untreated and plasma-treated polyamide 6

Plasma time (min)	Atomic concentration %		
	O 1s	N 1s	C 1s
0	11.96	10.6	77.45
15	20.22	10.24	69.54
30	22.47	9.99	67.54
45	22.07	8.71	69.23
60	22.91	8.33	68.76

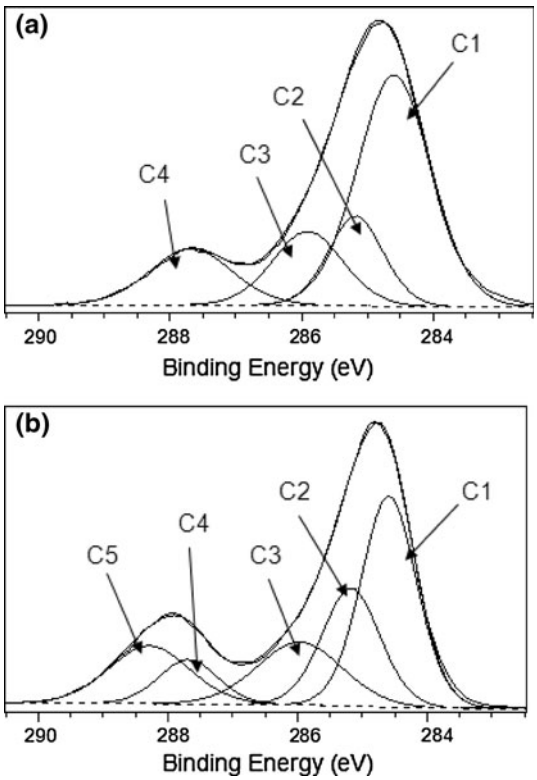

Fig. 1 XPS C 1s spectra of **a** untreated polyamide 6 and **b** polyamide 6 treated with 60 min of oxygen plasma

288.3 eV and is attributed to the carbonyl carbon of acids and esters [19–22].

Previous studies have shown that when polymer surfaces were subjected to plasma, oxidation would take place, thus leading to the formation of carboxylic acid, ester, ketone, and alcohol groups [18, 23, 24]. As the carbonyl carbon of ketone (O = *C*–C) has a similar chemical shift as the amide carbon [20], it would contribute to the intensity of the C4 peak. The carbons bonded to these newly formed carbonyl groups would then contribute to the intensity of the *C*2 peak. The formation of alcohol groups will also increase the intensity of the C3 peak. Table 2 summarizes the binding energy and relative percentage of C1s peaks for untreated and plasma-treated surfaces. After plasma treatment, it is observed that the relative amount of C1 and C4 decrease, while the amount of C2, C3, and C5 increase.

Figure 2 shows the ATR spectra of the untreated and plasma-treated PA films in different infrared regions. Some differences could be observed in the spectra of PA after plasma treatment. Firstly, from Fig. 2a, a shoulder appears in the region from 1680 to 1700 cm^{-1}, and its intensity increases with increasing plasma duration. This shoulder is attributed to the carbonyl groups formed from oxidation reactions [25–27]. This is consistent with XPS results. From Fig. 2b, it is observed that the two peaks in the region from 1350 to 1310 cm^{-1} increase with plasma treatment

Table 2 Binding energy and relative percentage of different chemical components of C 1s for untreated and plasma-treated polyamide 6

Plasma time (min)	C1		C2		C3		C4		C5	
	B.E. (eV)	%	B.E. (eV)	%	B.E. (eV)	%	B.E. (eV)	%	B.E. (eV)	%
0	284.6	53.49	285.19	15.64	285.91	16.31	287.67	14.56	–	–
15	284.6	33.47	285.18	25.58	286.02	16.04	287.71	8.76	288.33	16.16
30	284.6	30.21	285.21	27.15	286.08	15.55	287.71	5.79	288.30	21.30
45	284.6	33.11	285.21	24.69	286.05	17.82	287.70	5.74	288.31	18.65
60	284.6	37.52	285.19	22.03	285.99	17.13	287.69	8.38	288.30	14.95

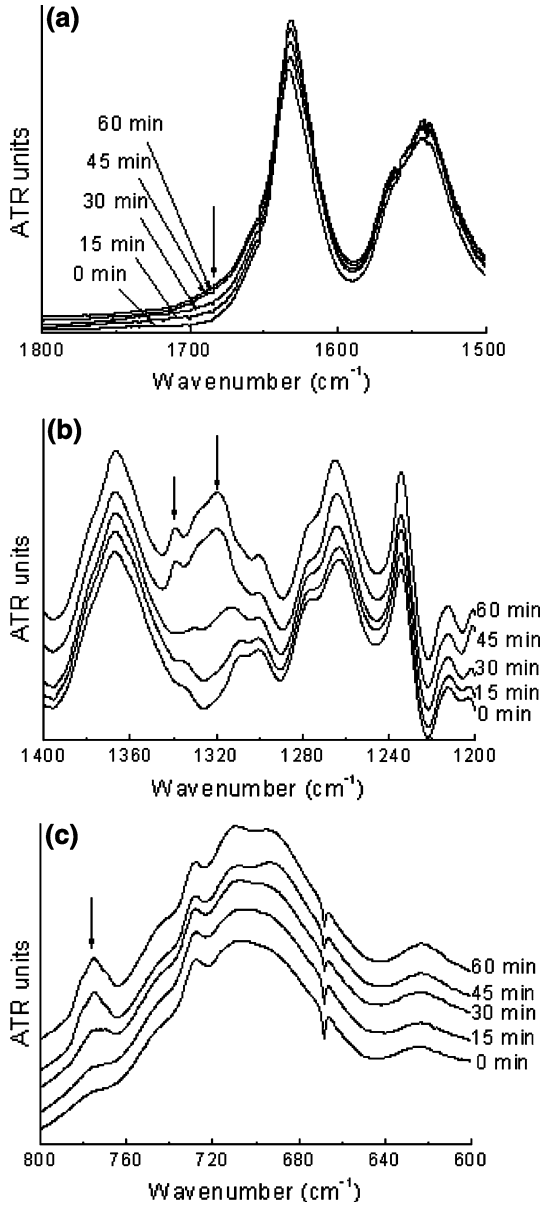

Fig. 2 ATR spectra of untreated and plasma-treated polyamide 6 films in different regions: **a** 1500–1800 cm^{-1}, **b** 1200–1400 cm^{-1}, and **c** 600–800 cm^{-1}

time. These peaks are attributed to the C–N stretching vibration region of *cis*-amides [26, 27]. From Fig. 2c, it is observed that a peak in the 790–750 cm^{-1} region increases in intensity with plasma time. This peak is attributed to the N–H wagging vibration of *cis*-amides [27].

Generally, PA molecules exist in the *trans* configuration, while the *cis* configuration exists mostly in cyclic amides with ring sizes having less than eight atoms [27]. The appearance of *cis* peaks after plasma treatment indicates the formation of cyclic amides on the surface.

Plasma-treated polyamide 6 nanocomposites

Table 3 shows the XPS analysis results of the plasma-treated polyamide 6 nanocomposites containing 2 wt% nanoclay (PC2). As all the plasma-treated nanocomposites had similar composition, only the data for PC2 is presented. In the nanocomposites, since silicon is a major component of nanoclay, its atomic concentration is representative of the relative content of MMT on the surface. Before plasma treatment, the Si concentration is only 0.39%. However, after the surface was exposed to oxygen plasma for 15 min, Si concentration increased significantly to 13.41%. As plasma treatment was increased further, Si concentration continued to increase but at a much smaller rate. The changes in the atomic concentration of carbon,

Table 3 XPS analysis of untreated and plasma-treated polyamide 6 nanocomposite containing 2 wt% nanoclay (PC2)

Plasma time (min)	Atomic concentration %			
	O 1s	N 1s	C 1s	Si 2p
0	11.91	10.56	77.15	0.39
15	42.46	4.86	39.27	13.41
30	43.47	3.58	37.44	15.51
45	45.31	2.09	35.02	17.58
60	46.68	2.01	33.14	18.17

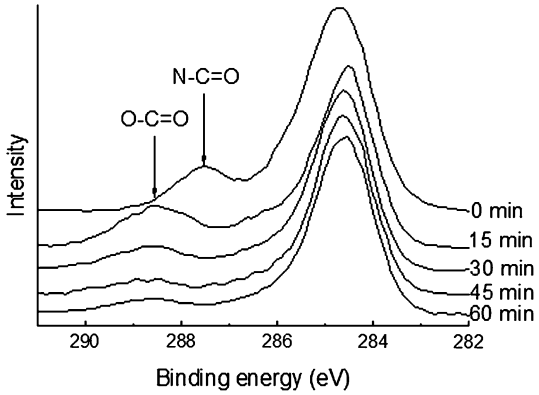

Fig. 3 XPS C 1s spectra for untreated and plasma-treated PC2

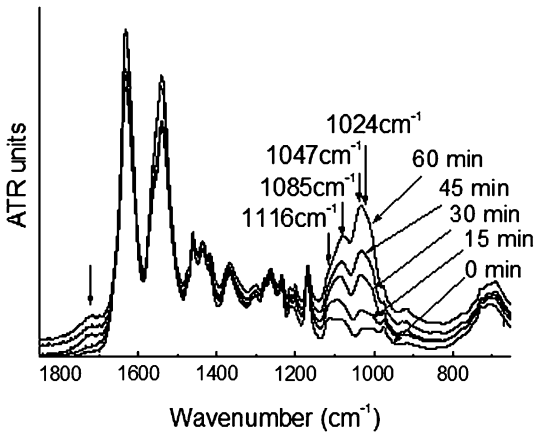

Fig. 4 ATR spectra of untreated and plasma-treated NC2

oxygen and nitrogen are similar to PA, i.e., that of oxygen increases while those of carbon and nitrogen decrease.

Figure 3 shows the XPS C 1s spectra for PC2 samples at different plasma treatment times. It is observed that the C4 peak at 287.7 eV, which belongs to the carbonyl carbon of the amide group, has disappeared after plasma treatment. A new peak at 288.3 eV, which is attributed to the carboxyl carbon of acid or ester groups, has appeared. The intensity of this peak decreases with increasing plasma duration.

Figure 4 shows the ATR spectra for PC2 with and without plasma treatment. Montmorillonite has four absorbance peaks arising from the Si–O stretching vibrations in the 940–1140 cm^{-1} region, namely at 1116, 1085, 1047, and 1024 cm^{-1} [28]. As shown in Fig. 4, the intensities of the Si–O stretching peaks at 1024 and 1085 cm^{-1} increase substantially with increasing plasma treatment time, implying an increasing concentration of nanoclay on the surface. This result is different from XPS which shows that surface Si concentration only increases slightly with increasing exposure to plasma. The reason for this difference is that XPS could only probe the nanocomposite or pure polymer surface up to a depth of only several nanometers whereas the penetration depth of infrared is around 1.5 μm. While the topmost few nanometers of the surface have reached a somewhat steady state clay concentration, the plasma was still causing compositional changes well below the surface even after 1 h.

Figure 4 also shows the appearance of a new peak at 1720 cm^{-1} in the plasma-treated nanocomposite. The intensity of this peak increases with plasma treatment time firstly and becomes relatively unchanged after 30 min. This is attributed to the carbonyl groups formed due to the oxidation process. The position of this carbonyl peak, however, is different from that of plasma-treated polyamide 6. This indicates that different types of carbonyl groups are formed on PA surface and nanocomposites surface. Furthermore, no infrared absorbance peaks due to *cis*-amide groups are observed for PC2 and nanocomposites with other MMT content.

Abrasion resistance

Figure 5 shows the abrasion results for polyamide 6 and its nanocomposites. For the samples without any plasma treatment, it is observed that the abrasion resistance decreases with clay content. These results are consistent with other literature reports [6]. The plasma-treated polyamide 6 has better abrasion resistance compared to the untreated material as well as all the plasma-treated nanocomposites. The optimal plasma treatment time for surface-modified PA is 15 min and the abrasion resistance decreases with increasing exposure. For PC2, PC4, and PC6, a plasma duration of 15 min resulted in better abrasion resistance than the respective untreated nanocomposites. Increasing the plasma treatment time led to poorer abrasion resistance. For PC8, all the plasma-treated surfaces perform worse than untreated PC8. Among all the nanocomposites, plasma-treated PC2 has the best abrasion resistance. In fact, PC2 exposed to 15 min of

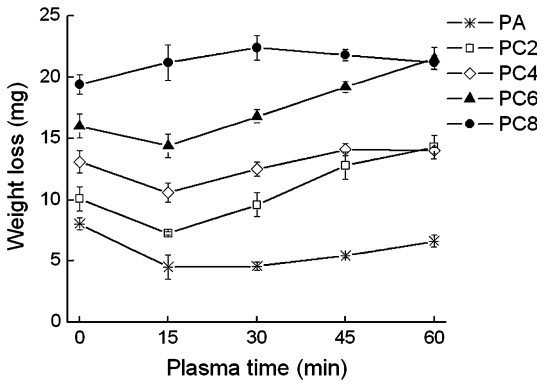

Fig. 5 Abrasion results of untreated and plasma-treated polyamide 6 and its nanocomposites

oxygen plasma has better abrasion resistance than pure polyamide 6.

Water contact angle measurements

The water contact angle measurement was conducted after stabilizing the sample in air for 1 day and stored for 1 month. Figure 6a shows the water contact angle of untreated polyamide 6 which is 64°. All plasma-treated polyamide 6 were fully wetted, i.e., their water contact angles were 0° even after 1 month, as shown in Fig. 6b. This implies that the surface of plasma-treated polyamide 6 was stable.

Oxygen plasma treatment has been found to improve the wettability of polymer surface due to the functionalization reactions which induced polar groups [38, 42, 43]. However, the hydrophilicity will generally recover to a certain extent during storage due to post-reaction [12] or reorientation of the polarity groups [29, 30]. The stability of the plasma-treated polyamide 6 surfaces indicates the presence newly formed chemical species which will not react in air and has

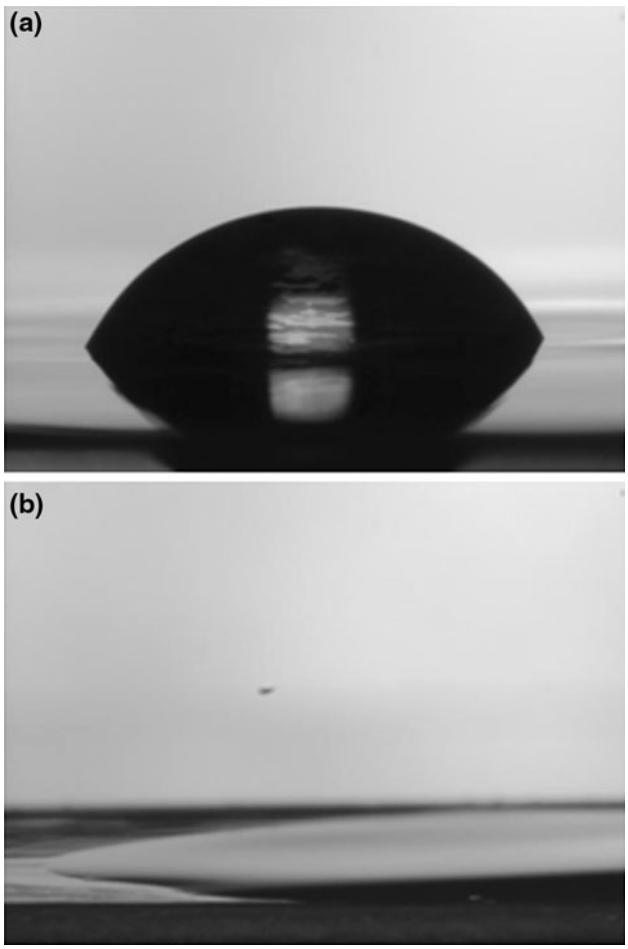

Fig. 6 Image of water contact angle for **a** untreated and **b** plasma-treated polyamide 6

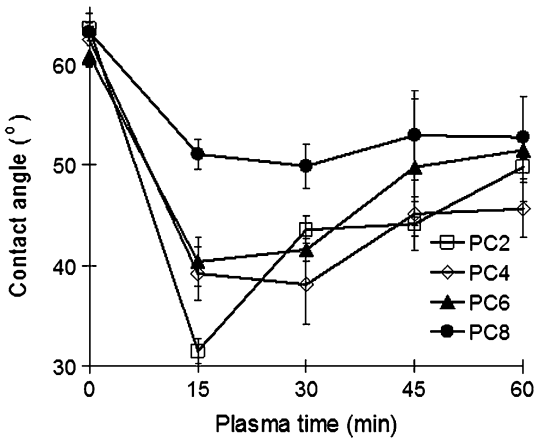

Fig. 7 Water contact angle measurements for untreated and plasma-treated polyamide 6 nanocomposites

good water solubility. This is consistent with ATR analysis (Fig. 2a, c) which shows cyclic *cis*-amides being formed on the surface of plasma-treated polyamide 6.

The water contact angles for nanocomposites samples are shown in Fig. 7. Before plasma treatment, the water contact angles were all around 60°. After plasma treating and storage for 1 month, the contact angles were reduced. After 15 min of plasma treatment, the contact angle decreased to between 30° and 40° for PC2, PC4, and PC6. Further exposure to plasma caused the contact angle to increase to around 50° in these samples. For PC8, the contact angles for plasma-treated samples remained at a relatively constant value of 50°.

Plasma reaction mechanisms on pure polyamide 6 surface

Based on the experimental results, we propose the reaction mechanisms shown in Fig. 8. Different kinds of free radicals can be formed once PA is exposed to the plasma phase. In Reaction 1, chain scission occurs at the C–C bond and forms short fragments. This reaction can proceed further, resulting in the formation of smaller fragments. Reaction 4 shows how a fragment with one amide group and less than 8 carbon atoms can form a cyclic *cis*-amide [27], the existence of which was confirmed by ATR (Fig. 2b, c) results. The chain scission products can also react with oxygen radicals in the plasma phase to form oxidized products (Reaction 5) [31].

In Reaction 2, chain scission occurs at the C–N bond. The radicals formed in this reaction can also undergo further chain scission or oxidization reaction (Reaction 6).

In Reaction 3, the C–H bond is broken and the subsequent products can undergo cross-linking [32, 33] (Reaction 7) and oxidization (Reaction 8). The cross-linking can lead to increased surface hardness and stiffness

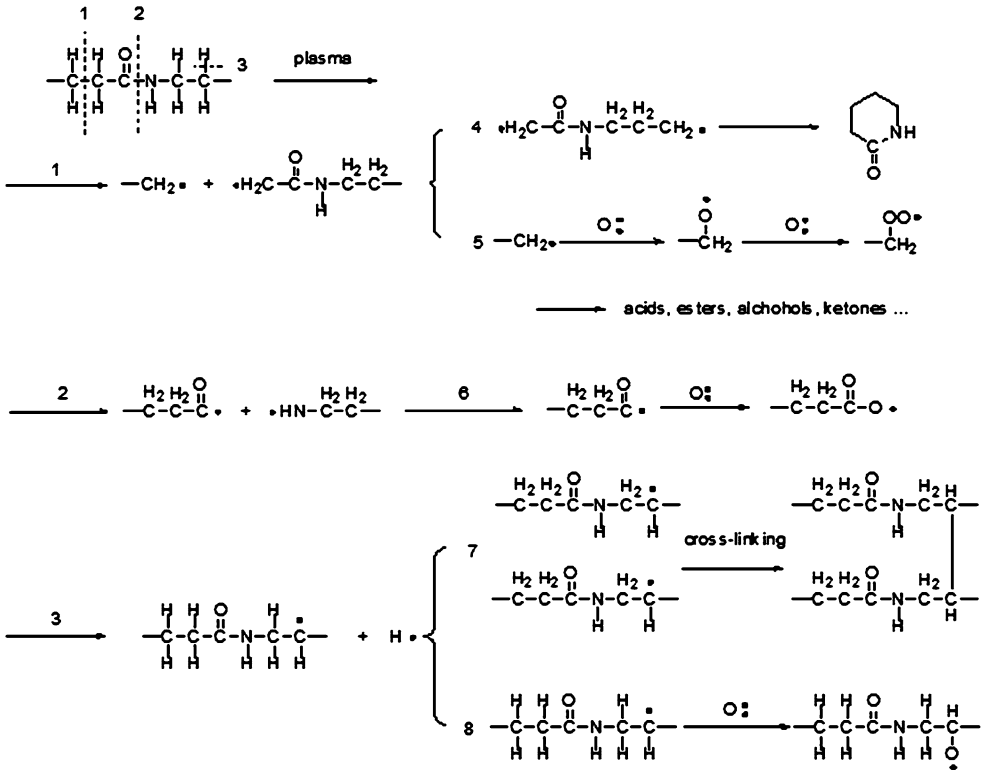

Fig. 8 Reaction mechanisms of polyamide 6 surface under oxygen plasma

[34], thereby enhancing the abrasion resistance of plasma-treated polyamide 6 [12, 34, 35]. However, the abrasion resistance of polyamide 6 is found to decrease with increasing plasma duration. This is because both cross-linking and chain scission reactions occur simultaneously during the plasma process [32, 36]. Chain scission reactions lead to degradation of the polymeric chain and formation of short chain fragments, which could be removed easily during the abrasion process. When chain scission reaction occurs on the network polymer chains, the network is broken and shortened. Furthermore, these short chains have been found to cross-link more easily [37], thus the network size formed by these chains would be smaller. Hence increasing plasma treatment leads to more cross-links but smaller network size. Besides cross-linking, the products of Reaction 3 can also undergo oxidization, as shown in Reaction 8.

As mentioned above, oxidation reactions occur during oxygen plasma treatment. Oxidation products have been observed by XPS analysis and ATR (Fig. 2a). Firstly, the atomic concentration of oxygen (Table 1) is observed to increase. This is attributed to the incorporation of oxygen atoms during the plasma reactions. The formation of acid groups was observed in XPS C 1s spectra (Fig. 1) and ATR spectrum (Fig. 2a). Further analysis of the relative percentage of different chemical components of C 1s for untreated and plasma-treated polyamide 6 has been presented in Table 2. In plasma-treated polyamide 6, the intensity of the new peak at C5 (O–C=O) and that of C2 (*C*–C=O) in the C 1s spectra are observed to increase simultaneously. Furthermore, the percentages of the C1 (C–C) and C4 (O=C–N or O=*C*–C) peaks are observed to decrease. However, the relative percentage of C3 (C–O/C–N) do not change much, thereby indicating that the oxidization process also results in the formation of hydroxyl groups on the surface. It is also observed that regardless of plasma treatment duration, XPS results show that the relative chemical compositions of the plasma-treated PAs are similar. Hence the polyamide 6 surface reaches an equilibrium state within 15 min. This phenomenon is commonly observed for plasma-treated surfaces and is referred to the "saturation state" of the surface [36].

Plasma reaction mechanisms on polyamide 6 nanocomposites surface

Chemical composition changes of the polyamide 6 nanocomposites due to plasma treatment have been analyzed by XPS. As shown in Table 3, the most significant changes in atomic concentrations occurred in the first 15 min of plasma treatment: Si and O increased while N and C decreased. Hence we propose that plasma modification of the nanocomposite surface occurs in two stages. Stage 1 is the rapidly etching of the organic component on the surface and occurs within the 15 min of plasma treatment during which the chemical composition changes significantly.

At the end of stage 1, the surface becomes enriched in clay as the organic components are removed by plasma [15]. In stage 2, the plasma continues to remove the polymer, but at a much slower rate, thereby leading to slower compositional changes at the surface.

From the C 1s spectra of PC2 shown in Fig. 3, it is observed that the peak attributed to amide groups disappears within 15 min and a new peak representing carboxylic carbons of acid or ester appears. The concentration of this peak decreases with time. These results show that there are at least two kinds of modifications occurring on the nanocomposite surface under oxygen plasma. One is oxidation reaction, resulting in the formation of carboxylic groups. The second is degradation which would lead to the disappearance of amide group and the reduction of carboxylic group with time. Such degradation can be catalyzed by organoclay [38, 39]. For polymers, degradation is usually initiated on functional groups, such as amide and carboxylic groups, and the rate of degradation is in the order: (CONH) > (COO–) > (CH2) [40]. This explains why the amide groups disappear fastest in the nanocomposites within 15 min of plasma treatment. Later, the newly formed carboxylic groups were also degraded. The degradation reaction would result in the formation of small segments, which can evaporate and extracted in the gaseous phase [41].

The increase in silicon concentration at the surface is due to clay aggregation as the organic components are removed due to degradation reaction. The increase in surface oxygen concentration may be attributed to two reasons. The first reason is the oxidization reaction of the remaining organic molecules on the surface. The second reason is due to the higher oxygen concentration in MMT compared to PA, hence oxygen content increases with clay content. However, based on the earlier C 1s spectra analysis, it is observed that the oxygen containing groups decrease with time, thus the second reason should be the reasonable one to account for the observed increase in oxygen concentration. Finally, as the carbon and nitrogen atoms are mostly derived from PA, thus their concentration changes are just opposite to that for silicon.

Based on XPS and ATR measurements, it is seen that PA is much more vulnerable than nanoclays in the plasma environment. Thus, the polymer chains are quickly etched away while nanoclay is left behind and would aggregate on the surface. The surface concentration of clay increases with plasma time, leading to a layer of clay rich region which is also increasing in thickness. However, it is observed that the abrasion resistance of PC2, PC4, and PC6 increased for short plasma treatment time but decreased with increasing plasma duration (Fig. 5), so that the best abrasion resistance is obtained at 15 min of plasma treatment. On the other hand, for PC8, the abrasion resistance is not improved at all regardless of plasma duration.

In a previous study of the abrasion resistance of polyamide 6 nanocomposites, we have shown that (a) the polymer matrix is easier to be removed than clay during the abrasion process and (b) in nylon 6/MMT systems, the poor abrasion resistance is attributed to defects at the clay–polymer interface, resulting in greater wear of the polymer matrix [8]. Based on the data in this paper, we propose a schematic for the surface modification of the nanocomposite as shown in Fig. 9. After the first stage of plasma treatment (i.e., the first 15 min), only the surface polyamide chains are removed, leaving behind a surface rich in clay. Such a surface would be more wear resistant [8]. In stage 2, the polymer segments are further degraded, including the inner polymer chains which are beneath the surface clay. This would lead to self-aggregation of the clay layers on top of the surface [15]. Such self-aggregated clay, however, would not be tightly bound to the polymer matrix and would be easily cut off by the abrader. This explains why nanocomposites with lower clay content that are not treated with plasma or treated with short durations of plasma have better abrasion resistance. For PC8, the effect of defects at the clay–polymer interface is preponderate over better wear resistance of clay [8], hence it is not possible to improve the abrasion resistance of PC8 regardless of plasma duration. Hence all the abrasion resistances of plasma-treated PC8 are similar or worse than PC8 without plasma treatment.

The water contact angles of PC2, PC4, and PC6 decrease after 15 min of plasma treatment, then increase again with plasma duration. The initial decrease in contact angle is attributed to an increase of surface hydrophilicity, which is due to the functional groups formed on the surface as a result of plasma oxidation. From the XPS C 1s spectra analysis, it is observed that the concentration change of carboxylic groups has the same trend as the water contact angle.

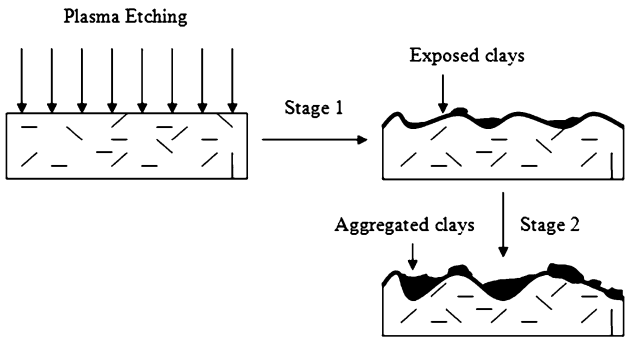

Fig. 9 Schematic illustration of plasma modification on polyamide 6 nanocomposite surface

Another factor that can affect the contact angle is nanoclay aggregation on the surface. As PC8 has the most nanoclay, its effect on contact angle is dominant. PC8 samples with different plasma treatment time all have contact angles of around 50°. For PC2, PC4, and PC6, their contact all tend to 50° with longer plasma duration. Hence the effect of nanoclay aggregation on contact angle will gradually dominate at long plasma treatment times. These observations indicate the contact angle of the polyamide surfaces treated with plasma will stabilize at around 50°.

Conclusions

Abrasion tests and water contact angle measurements were performed on commercial polyamide 6 and polyamide 6 nanocomposites. The surfaces of the materials were analyzed by FTIR-ATR and XPS.

In pure polyamide 6, plasma treatment led to the formation of cross-links and cyclic *cis*-amide species on the surface, thereby causing an increase in abrasion resistance and hydrophilicity, respectively.

In the plasma-treated polymer nanocomposites, the surface also became more hydrophilic due to oxidation and enrichment of clay at the surface. However, the plasma-treated nanocomposite surface is not as highly hydrophilic as that of plasma-treated homopolymer. Furthermore, an improvement in abrasion resistance was obtained in samples with low clay content when exposed to plasma for a short time. This is attributed to both cross-linking as well as the higher abrasion resistance of clay. However, longer exposure to plasma resulted in poorer abrasion resistance due to self-aggregation of clay particles which can be easily removed from the surface. It is observed that, with the exception of the nanocomposite with the highest clay content, there is an optimum duration ($\sim$15 min) of plasma treatment whereby pure polyamide 6 and the nanocomposites can achieve the best abrasion performance.

Our results show that oxygen plasma treatment can be used to modify polymer and polymer nanocomposite surfaces to enhance abrasion resistance. The best results are obtained at low clay content and an optimum plasma time. As polyamide 6 is widely used as an engineering plastic such as gears, one important implication of this work is that by introducing nanoclay into the polymer matrix and subjecting the nanocomposite to oxygen plasma, it is possible to enhance *both* the tensile properties and abrasion resistance of the resulting hybrid material. Understanding the effect of oxygen plasma on the polymer nanocomposite would facilitate the design of materials with "customized" surface properties for a wider range of applications.

Acknowledgements The authors thank Prof Mary Chan for the use of the plasma equipment. The authors also thank the Ministry of Education (Singapore) for funding this work.

References

1. Kojima Y, Usuki A, Kawasumi M, Okada A, Kurauchi T, Kamigaito O (1993) J Polym Sci Part A: Polym Chem 31:983
2. Pavlidou S, Papaspyrides CD (2008) Prog Polym Sci 33:1119
3. Nguyen QT, Baird DG (2006) Adv Polym Technol 25:270
4. Ray SS, Okamoto M (2003) Prog Polym Sci 28:1539
5. Liu TX, Liu ZH, Ma KX, Shen L, Zeng KY, He CB (2003) Compos Sci Technol 63:331
6. Srinath G, Gnanamoorthy R (2007) J Mater Sci 42:8326. doi: 10.1007/s10853-006-0165-x
7. Srinath G, Gnanamoorthy R (2006) Mater Sci Eng A 435:181
8. Zhou Q, Wang K, Loo LS (2009) J Appl Polym Sci 113:3286
9. Denes FS, Manolache S (2004) Prog Polym Sci 29:815
10. Li ZF, Netravali AN (1992) J Appl Polym Sci 44:319
11. Sanchis MR, Blanes V, Blanes M, Garcia D, Balart R (2006) Eur Polym J 42:1558
12. Hegemann D, Brunner H, Oehr C (2003) Nucl Instrum Methods Phys Res Sect B 208:281
13. Beake BD, Leggett GJ, Alexander MR (2002) J Mater Sci 37:4919. doi:10.1023/A:1020830717653
14. Zeuner M, Meichsner J, Poll HU (1995) Plasma Sources Sci Technol 4:406
15. Fong H, Vaia RA, Sanders JH, Lincoln D, Vreugdenhil AJ, Liu WD, Bultman J, Chen CG (2001) Chem Mater 13:4123
16. Wu TM, Wu CW (2005) J Polym Sci Part B: Polym Phys 43:2745
17. Wu TM, Yang SH (2006) J Polym Sci Part B: Polym Phys 44:3185
18. Pappas D, Bujanda A, Demaree JD, Hirvonen JK, Kosik W, Jensen R, McKnight S (2006) Surf Coat Technol 201:4384
19. Oh KW, Kim SH, Kim EA (2001) J Appl Polym Sci 81:684
20. Upadhyay DJ, Cui NY, Anderson CA, Brown NMD (2004) Colloids Surf A 248:47
21. Yip J, Chan K, Sin KM, Lau KS (2003) Appl Surf Sci 205:151
22. Errifai I, Jama C, Le Bras M, Delobel R, Gengembre L, Mazzah A, De Jaeger R (2004) Surf Coat Technol 180:297
23. Weibel DE, Vilani C, Habert AC, Achete CA (2007) J Membr Sci 293:124
24. Zhang W, Chu PK, Ji JH, Zhang YH, Jiang ZM (2006) Appl Surf Sci 252:7884
25. Morent R, De Geyter N, Leys C, Gengernbre L, Payen E (2008) Surf Interface Anal 40:597
26. Workman J (2001) Handbook of organic compounds: NIR, IR, Raman, and UV-Vis spectra featuring polymers and surfactants (a 3-volume set). Academic Press, Boston
27. Lin-Vien D (1991) The handbook of infrared and Raman characteristic frequencies of organic molecules. Academic Press, Boston
28. Ras RHA, Johnston CT, Franses EI, Ramaekers R, Maes G, Foubert P, De Schryver FC, Schoonheydt RA (2003) Langmuir 19:4295
29. Sanchis MR, Calvo O, Fenollar O, Garcia D, Balart R (2008) Polym Test 27:75
30. Drnovska H, Lapcik L, Bursikova V, Zemek J, Barros-Timmons AM (2003) Colloid Polym Sci 281:1025
31. De Jaeger R, Mazzah A, Gengembre L, Frere M, Jama C, Milani R, Bertani R, Gleria M (2008) J Appl Polym Sci 108:3191
32. PoncinEpaillard F, Vallon S, Drevillon B (1997) Macromol Chem Phys 198:2439

33. Bismarck A, Brostow W, Chiu R, Lobland HEH, Ho KKC (2008) Polym Eng Sci 48:1971
34. Dong H, Bell T (1999) Surf Coat Technol 111:29
35. Zhang RJ, Hager AM, Friedrich K, Song Q, Dong Q (1995) Wear 181:613
36. France RM, Short RD (1997) J Chem Soc Faraday Trans 93:3173
37. Yip J, Chan K, Sin KM, Lau KS (2002) J Mater Process Technol 123:5
38. Fornes TD, Yoon PJ, Paul DR (2003) Polymer 44:7545
39. Xu XF, Ding YF, Qian ZZ, Wang F, Wen B, Zhou H, Zhang SM, Yang MS (2009) Polym Degrad Stab 94:113
40. Prat R, Shi MK, Clouet F (1997) J Macromol Sci Part A Pure Appl Chem A34:471
41. Wheale SH, Barker CP, Badyal JPS (1998) Langmuir 14:6699
42. Garcia D, Sanchez L, Fenollar O, Lopez R, Balart R (2008) J Mater Sci 43:3466. doi:10.1007/s10853-007-2322-2
43. Lennon P, Espuche E, Sage D, Gauthier H, Sautereau H, Valot E (2000) J Mater Sci 35:49. doi:10.1023/A:1004728229418